

1112
20-20-100
1112

PRECIPITATION OF NiHfSi PHASE IN NiAl SINGLE CRYSTALS CONTAINING Hf

A. Garg, R. D. Noebe, and R. Darolia*

NASA Lewis Research Center, Cleveland, OH 44135

*General Electric Aircraft Engines, Cincinnati, OH 45215

Small additions of Hf to NiAl produce a significant increase in the high-temperature strength of single crystals¹. Hf has a very limited solubility in NiAl and in the presence of Si, results in a high density of G-phase ($\text{Ni}_{16}\text{Hf}_6\text{Si}_7$) cuboidal precipitates and some G-platelets in a NiAl matrix². These precipitates have a F.C.C structure and nucleate on $\{100\}_{\text{NiAl}}$ planes with almost perfect coherency and a cube-on-cube orientation-relationship (O.R.). However, G-phase is metastable and after prolonged aging at high temperature dissolves at the expense of a more stable Heusler (β' - Ni_2AlHf) phase. In addition to these two phases, a third phase was shown to be present in a NiAl-0.3at. % Hf alloy, but was not previously identified (Fig. 4 of ref. 2). In this work, we report the morphology, crystal-structure, O.R., and stability of this unknown phase, which were determined using conventional and analytical transmission electron microscopy (TEM).

Single crystals of NiAl containing 0.5at. % Hf were grown by a Bridgman technique. Chemical analysis indicated that these crystals also contained Si, which was not an intentional alloying addition but was picked up from the shell mold during directional solidification. These ingots were homogenized for 50h at 1590K and then furnace-cooled at an approximate rate of 10K/min in Ar. Samples for TEM were prepared by electropolishing^{1,2} and microstructural characterization and crystallographic analysis were conducted in a Philips 400T TEM operating at 120kV.

A bright-field image close to a $\langle 001 \rangle_{\text{NiAl}}$ zone-axis is shown in Fig. 1. The microstructure consisted of two types of precipitates which were distinctly different in size, morphology, and density. The high density of fine cuboidal precipitates (size ~ 10 -50nm) with $\{001\}_{\text{NiAl}}$ habit-plane (H.P.) were identified as the G-phase precipitates. The second type of precipitates had a noticeably lower density but their size was ~ 10 times larger than that of the G-phase. EDXS showed these precipitates to be rich in Hf and Ni and to contain some Si. In order to identify the crystal structure of these larger precipitates, several low-index microdiffraction (MBED) patterns were recorded from individual precipitates. These patterns could be indexed unambiguously as arising from the orthorhombic NiHfSi phase with unit-cell parameters $a = 0.64\text{nm}$, $b = 0.39\text{nm}$ and $c = 0.72\text{nm}$ and having the space group Pnma ³. Trace analysis indicated that these precipitates have a $\{111\}_{\text{NiAl}}$ H.P. When viewed along a $\langle 110 \rangle_{\text{NiAl}}$ zone-axis, two sets of edge-on NiHfSi precipitate plates on the $\{111\}_{\text{NiAl}}$ planes parallel to the beam and two other sets inclined 35° w.r.t. the beam were clearly visible (Fig. 2). In a $\langle 111 \rangle_{\text{NiAl}}$ zone-axis, the NiHfSi precipitate plates had a rectangular morphology with sides parallel to $\langle 110 \rangle_{\text{NiAl}}$ and $\langle 112 \rangle_{\text{NiAl}}$ directions. MBED from these plates showed superimposed precipitate and matrix spots which suggested an O.R. given by $(100)_{\text{NiHfSi}} \parallel (111)_{\text{NiAl}}$, $[010]_{\text{NiHfSi}} \parallel [101]_{\text{NiAl}}$, $[001]_{\text{NiHfSi}} \parallel [121]_{\text{NiAl}}$ (Fig. 3). Since there are three equivalent $\langle 110 \rangle$ directions in a $\{111\}_{\text{NiAl}}$ plane, there are 3 variants of NiHfSi precipitate in each $\{111\}_{\text{NiAl}}$ plane (as shown in Fig. 3) for a total of 12 variants possible in the NiAl matrix. Common symmetry elements (2/m) and symmetry considerations of the precipitate and NiAl lattices also predict a rectangular morphology and a total of 12 variants for the NiHfSi phase. In each variant, preferential growth was along the $[001]_{\text{NiHfSi}} \parallel \langle 112 \rangle_{\text{NiAl}}$ direction, along which the misfit was least (0.6%) and the corresponding planes $(001)_{\text{NiHfSi}}$ and the $\{112\}_{\text{NiAl}}$ were exactly parallel. Aging experiments indicated that NiHfSi phase is not a stable phase in this particular alloy and on aging at 1300K for 10h, it begins to dissolve in favor of the β' phase (Fig. 4).

References

1. I.E. Locci, R. Dickerson, R.R. Bowman, J.D. Whittenberger, M.V. Nathal, and R. Darolia, *MRS Symposium Proceedings* 288(1993)685.

2. I.E. Locci, R.D. Noebe, R.R. Bowman, R.V. Miner, M.V. Nathal, and R. Darolia, *MRS Symposium Proceedings* 213(1991)1013.

3. P. Villars and L.D. Calvert, *Pearson's Handbook of Crystallographic Data for Intermetallic Phases* (1991)3895.

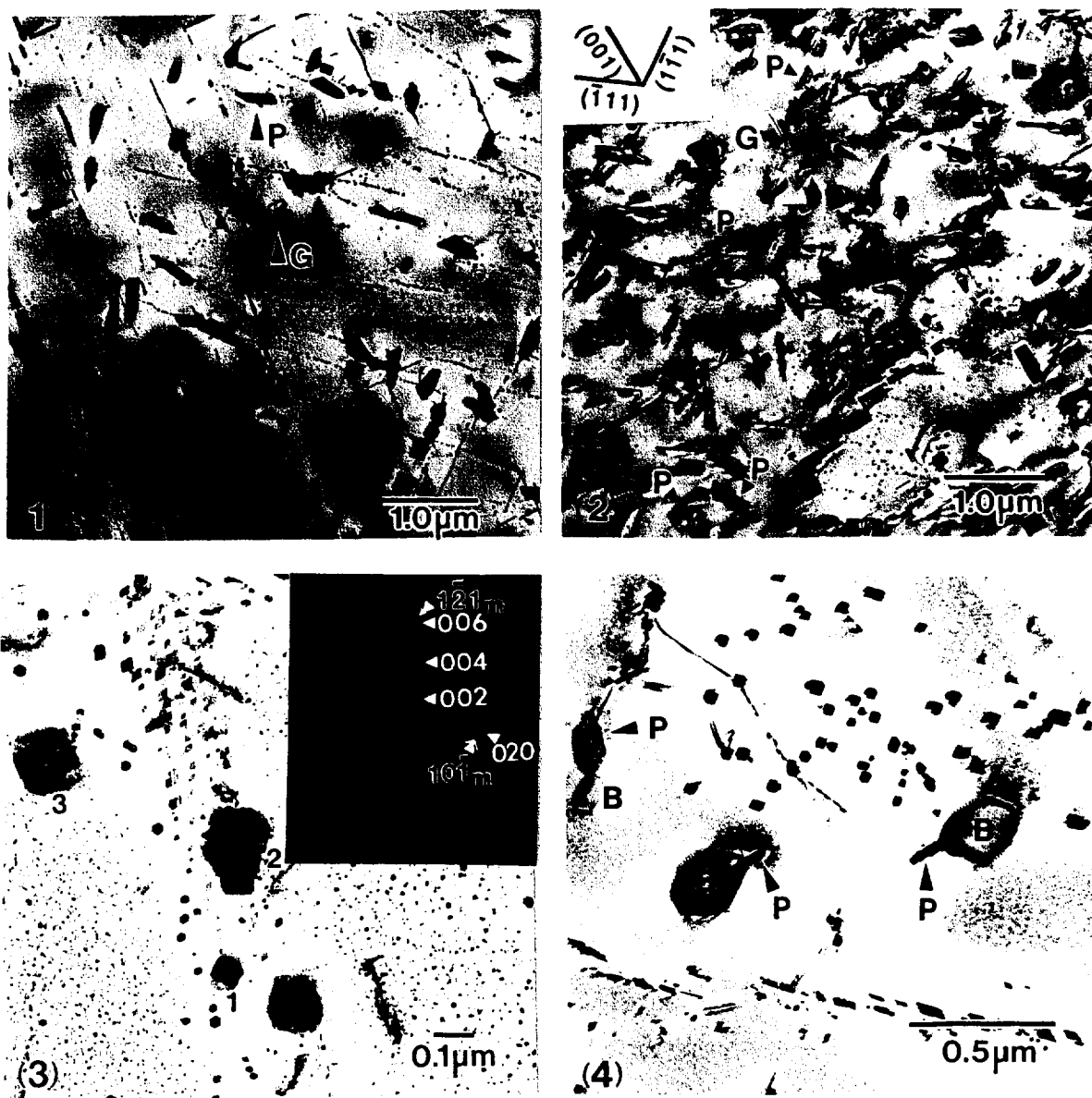


Fig. 1: A bright-field TEM image close to a $\langle 001 \rangle_{\text{NiAl}}$ zone-axis, showing precipitation of fine $\text{Ni}_{16}\text{Hf}_6\text{Si}_7$ (marked G) and relatively coarse NiHfSi (marked P) precipitates in a homogenized and furnace-cooled sample.

Fig. 2: A bright-field TEM image close to the $[110]_{\text{NiAl}}$ zone-axis showing formation of rectangular plates of NiHfSi phase formed on $\{111\}_{\text{NiAl}}$ planes.

Fig. 3: Transmission electron micrograph showing three variants of NiHfSi phase on a $\{111\}_{\text{NiAl}}$ plane. MBED along the $[100]_{\text{NiHfSi}} \parallel [111]_{\text{NiAl}}$ direction from plate 2 shows the O.R. between the NiHfSi phase and the NiAl matrix.

Fig. 4: Transmission electron micrograph showing the nucleation and growth of β' -precipitates (marked B) on the original NiHfSi plates in a sample aged at 1300K for 10h. Zone-axis $\sim \langle 110 \rangle_{\text{NiAl}}$.